Terr. Atmos. Ocean. Sci., Vol. 27, No. 4, 463-472, August 2016 doi: 10.3319/TAO.2016.01.01.01(ISRS)

Automatic Image Contrast Enhancement for Small Ship Detection and Inspection Using RADARSAT-2 Synthetic Aperture Radar Data

Jaehoon Jeong[1] and Chan-Su Yang[1, 2, 3, *]

[1] Marine Safety Research Center, Korea Institute of Ocean Science and Technology, Korea
[2] Department of Integrated Ocean Sciences, Korea University of Science and Technology, Daejeon, Korea
[3] Department of Convergence Study on the Ocean Science and Technology, Ocean Science and Technology School, Busan, Korea

Received 12 June 2015, revised 20 December 2015, accepted 1 January 2016

ABSTRACT

This study devises an automatic synthetic aperture radar (SAR) image enhancement method for ship detection and inspection for installation in a near-real-time automatic high-speed processing system. The proposed method was examined in small ship inspection and detection over the Ieodo Ocean area off Korea using RADARSAR-2 HV-polarization data. The proposed method involves four steps. First, the SAR input data is converted into a highly compressed gray scale image, which enables both computer screen display and high-speed processing due to its light volume. Second, the overall contrast is adjusted by power-law scaling to strengthen the target discrimination, which is attenuated because of the inefficiency of one-sided intensity distribution. This additionally provides excellent target visibility. Third, the intensity of the area in which targets and clutter coexist is rescaled from 0 to 255 using min-max linear stretching. This suppresses background clutter and makes targets more easily distinguishable from the clutter. Lastly, the remaining clutter is successfully eliminated using a median filter. As a result, an output image is obtained that is close to binary data and enables ship detection using only simple global thresholding. Our ship detection results were compared with that of ships identified using an automatic identification system and those visible in high-precision images by visual inspection. We verified that our method offers a high detection rate for small ships and does not involve complexity in distribution assumption, filtering or thresholding. The potential of our method is confirmed as an automatic SAR enhancement method for near-real-time ship detection and inspection.

Key words: Synthetic aperture radar, Ship detection, Contrast enhancement, Automation, Power-law scaling

Citation: Jeong, J. and C. S. Yang, 2016: Automatic image contrast enhancement for small ship detection and inspection using RADARSAT-2 synthetic aperture radar data. Terr. Atmos. Ocean. Sci., 27, 463-472, doi: 10.3319/TAO.2016.01.01.01(ISRS)

1. INTRODUCTION

In the last decade the remote sensing community has become increasingly interested in using synthetic aperture radar (SAR), also known as coherent microwave sensor, which enables ocean surveillance and monitoring under all weather conditions. SAR data have been adopted as a useful measure for ship detection, identification, and classification in ocean areas.

Several investigations have reviewed and validated the SAR potential for such applications (Ouchi et al. 2004; Margarit et al. 2006; Huang et al. 2009; Hwang and Ouchi 2010; Chaturvedi et al. 2012; Ouchi 2013).

In SAR imagery the object's appearance is severely disturbed by significant speckle noise and discontinuity effects. Speckle noise with a high backscattered response may be regarded as the target, whereas a target with an insufficient backscattered response may have very low visibility and be hard to detect. Therefore, image contrast enhancement that highlights targets and suppresses background clutter is essential for retrieving ship positions from SAR imagery. After such image enhancement, a method for determining the appropriate threshold is also required to distinguish the targets from clutter. Many studies have attempted to reduce the false-alarm rate and improve the ship detection rate through various denoising and image enhancing and thresholding approaches.

For example, Ouchi et al. (2004) proposed a ship detection algorithm based on coherence images derived from

* *Corresponding author*
E-mail: yangcs@kiost.ac

multi-look SAR image cross-correlation. Their method computes the cross-correlation values between two images extracted by moving small sized windows from the multi-look SAR intensity (or amplitude) images. It then produces a coherence image comprised of the cross-correlation values from the intensity images. Wang et al. (2008) proposed an improved constant false-alarm rate (CFAR) ship detection algorithm for SAR images based on the alpha stable distribution model. The existing CFAR algorithm, which is widely used for setting a threshold, employs the Gaussian or K-distribution. Wang et al. (2008), on the other hand, adopted the alpha-stable distribution for using CFAR. Their results verified the alpha-stable distribution advantage over the Gaussian or K-distribution for ship detection. Huang et al. (2009) proposed a method based on the coherence-reduction speckle noise (CRSN) algorithm and coherence CFAR detection algorithm. Their method reduced speckle noise for SAR images, enhanced the contrast between targets and background clutter via coherent SAR image processing and improved the detection ratio for SAR ship targets from the SAR imaging mechanism. Hwang and Ouchi (2010) suggested an approach using multi-look cross correlation (MLCC) and CFAR. They applied CFAR to coherence images produced by MLCC to improve the ship detection performance by SAR. Using this approach they could extract small fishing boats from phased array type L-band SAR (PALSAR) data. In addition, several algorithms have been suggested and validated for ship detection using SAR imagery (Kim et al. 2001; Margarit et al. 2009; Dubey et al. 2013).

Despite the above contributions, existing ship detection approaches typically involve complicated procedures and methods because they focus only on improving the target detection rate. This may not be suitable for commercial software that requires automatic high-speed processing. Data compression for high-speed processing and a simple method for automatic processing may be critical, particularly if the algorithm is to be implemented in commercial software for near-real-time detection and monitoring of ship targets using SAR imagery. Handling the original volume during full processing or including complicated filtering or thresholding may be obstacles to such software. Furthermore, it may be additionally important to provide a high-precision image with excellent visibility if any interest exists in inspecting targets on a computer screen from SAR imagery. For example, such precision images can be used to manually extract targets by human operators in case the algorithm fails to produce the desired outcome. In short, in addition to the target detection rate, many other important considerations should be made for a near-real-time ship inspection and detection system.

This paper proposes an automatic SAR image enhancement method that is focused on a near-real-time ship inspection and detection system. Our method aims to provide a high ship target detection rate without applying complex filtering or thresholding, which could be major obstacles to automatic or high-speed processing. In the proposed method a gray scale image is highly compressed from SAR input data for use in high-speed processing. The gray scale image is rescaled based on the power-law. A min-max linear stretching is then used to effectively perform target emphasis and background suppression through the overall brightness adjustment. The enhanced image is further processed using a simple median filter and global thresholding for extracting ships. The results are evaluated with visual inspection using ship positions obtained using automatic identification system (AIS). Power-law scaling that directly transforms from SAR input data into a high-precision image with excellent visibility for targets is further discussed. This study elucidates and validates the potential of our approach to automatically enhance SAR images for near-real-time ship detection and inspection.

The remainder of this paper is organized as follows. In section 2 we briefly describe the characteristics of the local test area that contained numerous small ships. In section 3 we outline the automatic SAR enhancement process for ship detection using RADARSAT-2 HV data, which includes the resulting images produced at each step. In section 4 the image enhancement process, with a focus on the visual target identification, is discussed. Our conclusions are presented in section 5.

2. TEST AREA

Our proposed image enhancement method was examined for the detection and inspection of ships distributed over the Ieodo Ocean area in South Korea using RADARSAT-2 Single Look Complex (SLC) data (HV-polarization images). In general, HV data is very useful for measuring ship detection. Compared with HH-polarization data, HV data provides a large radar cross-section (RCS) difference between the sea surface and ship targets (Ouchi 2013). This enables a target to be more easily distinguished from the HV data and fosters the effective utilization of HV data as input data for a near-real-time automatic ship inspection and detection system.

However, according to existing research, the test area contains numerous small ships, which may lead to difficulties in discriminating between targets and background clutter. This ship information was previously collected from the test area using the AIS receiver, which was installed on the Ieodo Ocean Research Station (IORS) for monitoring marine traffic and fishery activity in the jurisdictional sea area (Hong and Yang 2014). The chart in Fig. 1 was constructed by averaging ship data collected from 21 to 30 November 2013, including the acquisition time of the RADARSAT-2 data used in this work. The ship data collection results verify that many of the ships in the test area were of no discernible type or were fishing boats. These sea craft were therefore categorized as small ships.

More specifically, the ship position data collected by AIS over the test area at the SAR imagery acquisition time are shown in Fig. 2. Depicted on the left side of the image are the wind and water current speeds in the test area at the RADARSAT-2 Wide Beam Mode data acquisition time, as well as the data coverage. Strong winds and ocean current speeds were also observed from the satellite data in the test area, which may increase the background clutter effects (MetOp for wind, AVISO for water current). The right side of the figure depicts data on the weather condition within the SAR imagery coverage area. As shown, the vessels that are equipped with a Class-B type AIS transponder were a large proportion (approximately 80%) among the total vessels. This percentage supports the information that the RADARSAT-2 images used in this work contained many small targets whose responses may not have been sufficiently high. Overall, it was apparent that our test images contained strong background clutter effects as well as many small targets. Inspecting and detecting ships in such conditions is a challenging task, even for HV-polarization data. We therefore evaluated whether our automatic SAR enhancement method is effective under such conditions.

3. METHODOLOGY AND RESULTS

In this section the automatic SAR enhancement method process for ship detection using RADARSAT-2 HV data—including the resultant images produced at each step and the ship detection results—is described. Figure 3 depicts the proposed image enhancement procedure used in this study. The method is comprised of four steps. In the first step the SAR input data is converted into a physical quantity called the normalized RCS or backscattering coefficient, which is measured in decibel (dB) scales using logarithmic transformation. The data is then converted into a gray scale in the 0 to 255 range using linear transformation. In this step the SAR input data, whose volume is approximately 1 GB, is converted into a highly compressed gray scale image with a volume of approximately 60 MB to enable high-speed processing during the full procedure. It is apparent that such compressed data can be processed much faster than the original large data volume.

As shown in Fig. 4, a gray scale image can be displayed on the computer screen as an image containing dual-peak distributions for targets and background clutter, respectively.

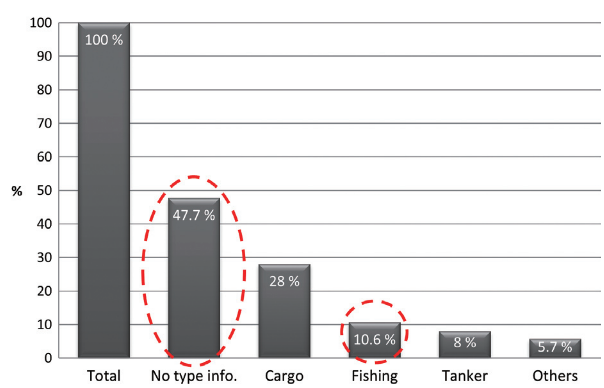

Fig. 1. Classification of ships in the Ieodo Ocean area from 21 to 30 November 2013. (Color online only)

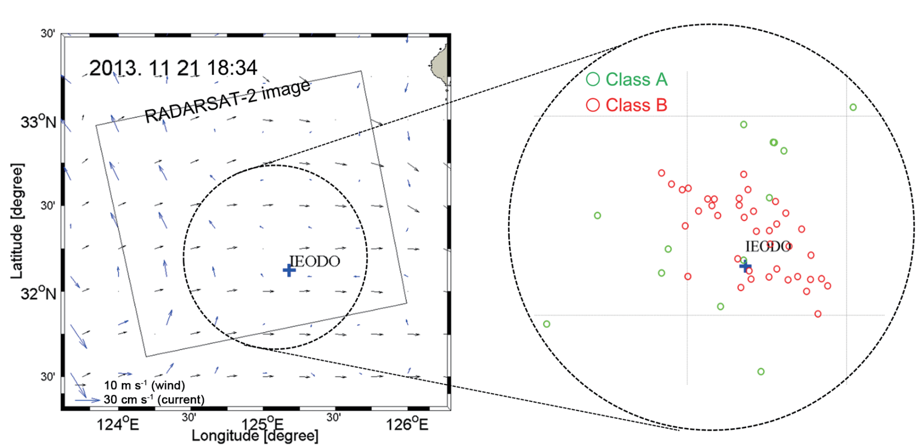

Fig. 2. Wind and water current speeds in the test area at RADARSAT-2 Wide Beam Mode data acquisition time, and the data coverage (left) and ship information collected by AIS (right). (Color online only)

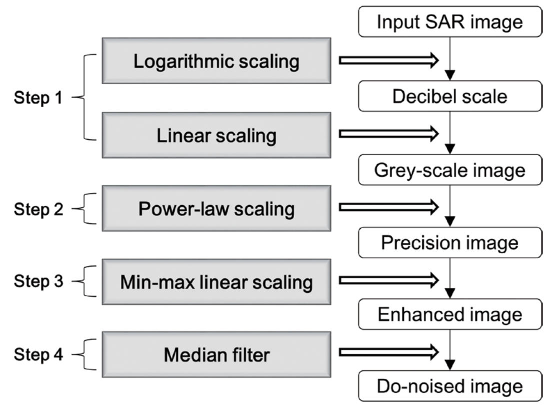

Fig. 3. Procedure for proposed automatic SAR image enhancement.

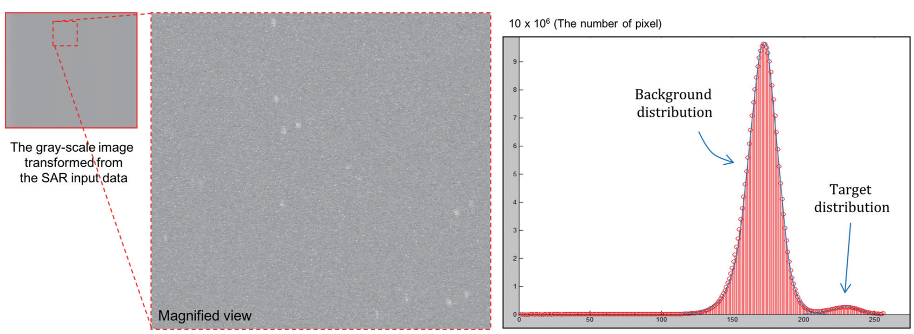

Fig. 4. Grayscale image (magnified view) and its intensity distribution. (Color online only)

The left panel of the figure presents a magnified view of a certain area while the right panel in the figure depicts a histogram drawn for the whole area using RADARSAT-2 HV data. The histogram is very smooth and ideal with a dual-peak distribution. However, the image has low visibility for targets due to the inefficiency of single-sided distribution. The overall brightness being relatively high may additionally be explained by strong winds and current speeds, as confirmed in Fig. 2. In the second step power-law scaling based on Eq. (1) is applied to the gray scale image for retrieving target discrimination that is attenuated. The power-law was mainly addressed to explain the input-output characteristics of the cathode ray tube (CRT) display; moreover, it has been utilized more frequently to improve image contrast in human or computer vision (Huang et al. 2013). Here, we adopted it for SAR image enhancement and verified its potential for handling SAR images. It efficiently performs image visibility enhancement by stretching the one-sided intensity distribution of the gray scale image.

In this step the statistical values for a bimodal distribution are pre-calculated for effective image-stretching. For automatic mean and standard deviation (STD) calculation for each distribution, it is assumed that both distributions are normally distributed. Although the value derived from such assumption may not be exactly true, only a slightly biased value (which will not make an appreciable difference in the final results) is expected to be obtained when carefully observing the histogram, as in Figs. 4 and 5. For automatic and high-speed processing (that is our primary concern), such an assumption seems to be positively necessary on the grounds that it does not produce a great error. However, such assumption needs to be more carefully reviewed when focusing on the detection accuracy rather than automation or speed because the pixel intensity distribution may depend on the test image used or the density of targets and background clutter. Under such assumption the mean values can be obtained at the peak for each distribution, while STD can be calculated using half of the total for each distribution; e.g., using values lower than the mean in the case of background distribution, or using values higher than the mean in the case of target distribution. Figure 5 shows the histogram details in Fig. 4 and presents the range of intensity values for targets and background clutter, respectively, with the assumption that most of the data (approximately 99.7%) are within three STDs of the mean. This represents the range in which the intensities coexist.

$$P_{output} = C \cdot P_{input}{}^{\exp},\ C = 125 / mean(P_{input}{}^{\exp}) \\ (\text{if } P_{output} > 255,\ P_{output} = 255;\ \text{if } P_{output} < 0,\ P_{output} = 0) \quad (1)$$

The images rescaled using the power-law with different exponent values and their intensity distributions are shown in Fig. 6. It can be confirmed that the power-law scaling gives greater prominence to targets. The higher the exponent is, the brighter the target is. However, an appropriate exponent must be selected to avoid some clutter being categorized as targets; i.e., too high an exponent may highlight even the clutter as well as the targets. For example, one must be careful to not exceed 255 in the output value corresponding to the value of $mean_b + 3\sigma_b$. In this work the value of the exponent was determined to be 3.0, whose adequacy can be validated by checking whether the output value of $mean_b + 3\sigma_b$ by Eq. (1) is greater than 255. Nevertheless, the optimal exponent depends on the SAR imagery used.

In the third step min-max linear scaling is applied to the power-law scaled image. This scaling mainly performs background suppression. The values less than the designated minimum value (e.g., $mean_t + 3\sigma_t$) are converted to zero based on the assumption that intensities lower than the minimum value do not contain the target intensity. In this step the intensities of the area where targets and clutter coexist are expanded from 0 to 255, as shown in Fig. 7a. This allows realizing effective separation between the targets and background clutter and therefore makes targets more easily distinguishable from clutter, as demonstrated in Fig. 7b.

In the last step the remaining clutter in the image is eliminated using a 2D median filter with 5 × 5 pixel window size. We confirmed that a larger window size leads to a smaller number of detected targets. The optimum window size was determined after testing various window sizes. While previous methods listed in introduction used adaptive filtering or another filtering method with complexity, our method employs only a median filter which is one of the simplest filters. It is apparent that there will be significant differences between the two types of filters, in terms of memory and time. Figure 7c shows the image denoised using the median filter. Because there only intermittent clutter exists in the image enhanced during the first to third steps (Fig. 7b), the output image using the median filter can be obtained close to binary data, which enables ship detection using global fixed thresholding. Figure 8 represents magnified views of the resulting images generated at each step. The first graphic shows the gray scale image that was highly compressed in the first step. In the second graphic the image was rescaled based on the power-law at the second step. In the third graphic the image has been linearly scaled using min-max values in the third step. In the fourth graphic the image has been denoised, and as a result, almost binarized by the median filter in the fourth step. All procedures were performed automatically.

The ship detection result was easily achieved from the binary image in the final step. The ship positions were plotted onto the screen, as shown in Fig. 9. The size of an individual detected ship is estimated roughly based on the image resolution, which is also shown. In total, 325 ships were extracted. It is clearly verified that many small ships could be extracted over the area. The results validate that our enhancement method can be very effective for ship detection, including small ones.

The ship detection results were compared to ship position information collected by AIS whose positional accuracy is estimated to be approximately 0.0001 minutes for both latitude and longitude, as shown in Fig. 10. The ship positions by AIS were presented with two categories: one that coincides with the SAR ship detection results and the other that does not. It is well confirmed that our results coincide with those by AIS, showing that among the total ship data collected by AIS, above 80% of the ships were confirmed detected by our method, considering a slight difference due to a lack of geometric SAR correction or position matching between the two data sets. Many ships contain small targets not collected by AIS were additionally detected by our method. One may ask if these are false-alarm errors. However, we must note that many small ships that may not have been perceived by AIS were distributed over our test area. Although a more thorough evaluation remains, e.g., more rigorous comparison based on the geometric SAR imagery correction and position and time matching between SAR and AIS, our results shown in Fig. 10 clearly demonstrate our method's high detection rate for ships, particularly in the case of small ships. We further evaluated our results by visual inspection using high-precision images that provide high-visibility for targets. This is addressed in the next section.

Unlike the previous studies mentioned in section 1, which adopted complex distribution assumptions (e.g., log-normal distribution for clutters or Rayleigh distribution for targets), denoising filters (e.g., adaptive median, or Wiener or bilateral filters), or thresholding (e.g., locally adaptive or hysteresis thresholding), our enhancement method does not require complex algorithms. It enables the detection of small ships in SAR images by simply using a median filter and global fixed thresholding. The proposed method is a near-real-time automatic practical use process. Our method showed outstanding performance in small ship detection.

4. IMAGE ENHANCEMENT FOR HIGH-VISIBILITY TARGETS

In most cases the human eye can intelligently recognize the presence of targets owing to its capability to perceive an image in a multiscale manner, even in the case of a small target whose backscattered response is not sufficiently high. A high-precision image with excellent object visibility can play an important role in ship identification using a human operator. One may consider the use of such an image for manually extracting targets in the case small ships undetected by automated algorithms. Such an image may be used for evaluating the results of a target detected by a particular

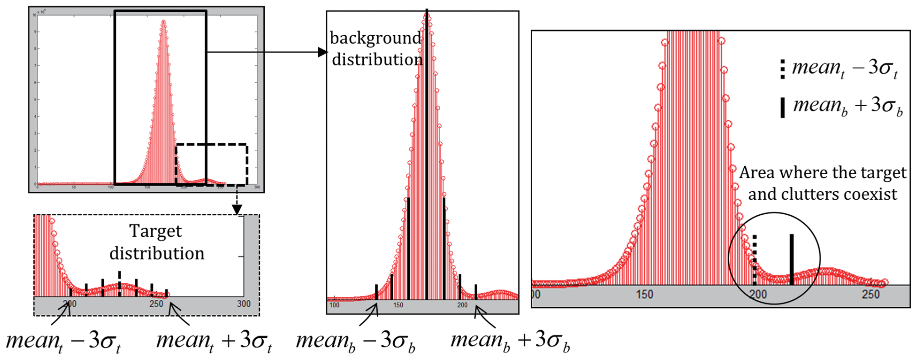

Fig. 5. Ranges of intensity for targets and background clutter. (Color online only)

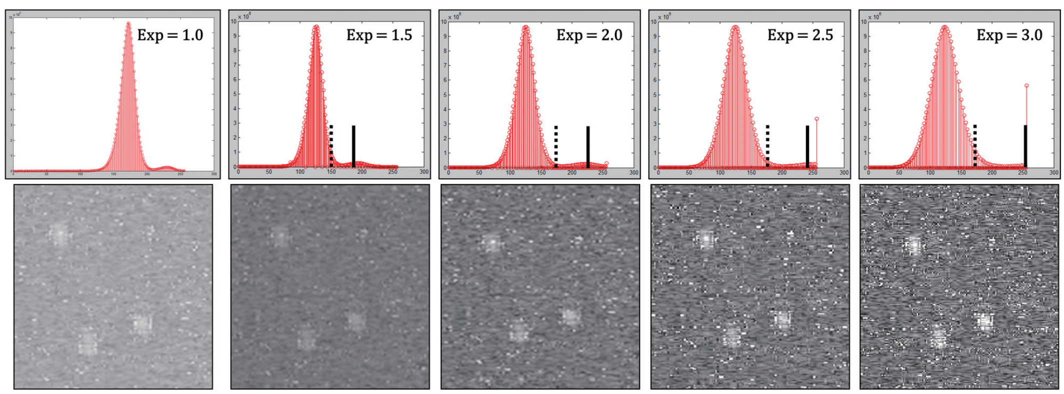

Fig. 6. Resultant images and their histograms according to different exponent values. (Color online only)

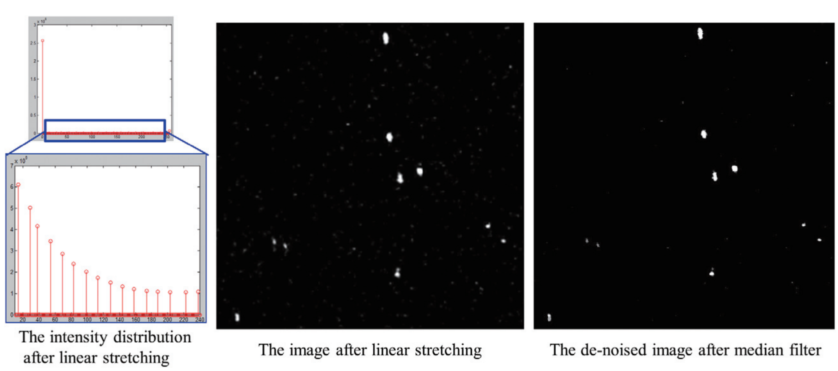

Fig. 7. Intensity distribution and image by min-max linear stretching and the image denoised by the median filter. (Color online only)

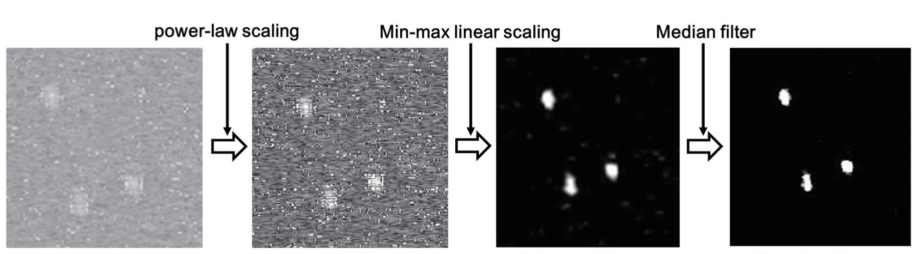

Fig. 8. Magnified views of the image generated at each step.

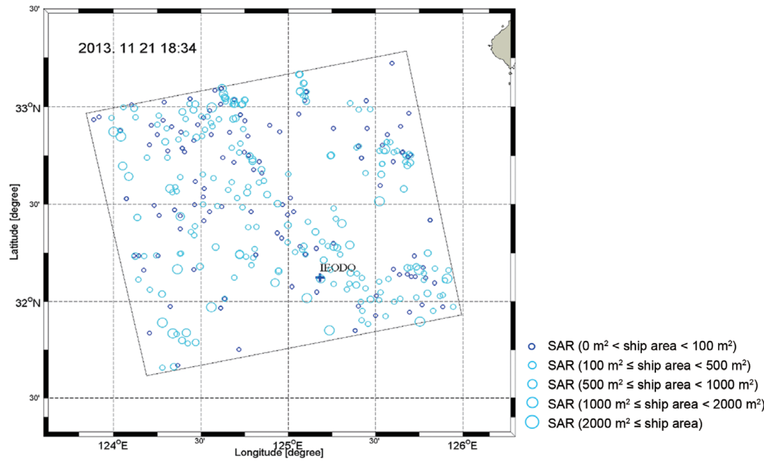

Fig. 9. Ship detection results from RADARSAT-2 data using our enhancement method. (Color online only)

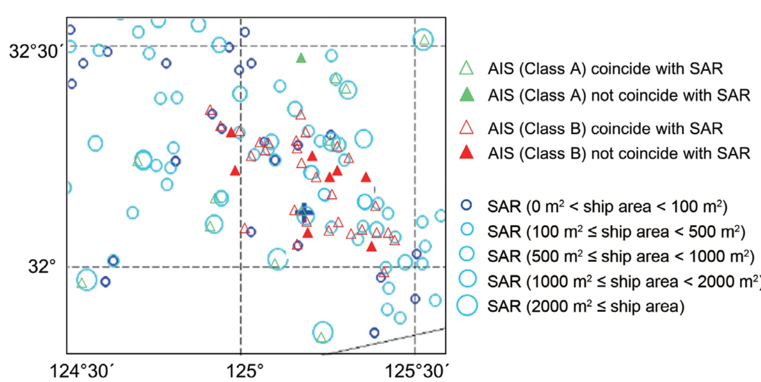

Fig. 10. Comparison of ships detected by our method and those collected by AIS. (Color online only)

algorithm by accounting for the difficulties in achieving target reference positional information in SAR imagery. No previous studies have discussed the importance of this image type for inspecting targets or evaluating results. In this section, we discuss image transformation that is focused on high-visibility for targets and use of the resultant image for evaluating ship detection results.

We adopted the power-law transformation to generate the gray scale of a high-precision image with excellent target visibility from the SAR input data. This approach is based on the fact that human vision follows the power-law function; that is, it has a greater sensitivity to relative differences between darker tones than between lighter ones. In the enhancement method described in the previous section, the power-law was used only to enhance the contrast of the gray scale image. Here, power-law scaling is used to directly convert the SAR input data into a high-precision image for ship recognition. We believe that this direct conversion using power-law transformation can provide excellent target visibility. It can therefore be very useful in accurately displaying an image on a computer screen and visually inspecting the targets, particularly in the case of small targets. In terms of commercial software such a capability may be significant and useful.

Figure 11 shows magnified views of a high-precision image that was directly transformed from the SAR input data using Eq. (1) based on the power-law. Here, the value of the exponent was 0.35. However, the optimal exponent depends on the SAR imagery used. As shown by the figure, it is evident that the image provides high visibility for target recognition, compared to the gray scale image (Fig. 4) obtained using logarithm and linear scaling. This supports the potential of power-law scaling for direct transformation from an original SAR input data into a high-precision image with excellent target recognition visibility.

As mentioned above, in our enhancement method, power-law scaling was used only to enhance the gray scale image. It was not adopted for gray scale image generation. This is because this direct transformation is missing some important characteristics, such as double-peak distribution for targets and clutter, as confirmed in the Fig. 11 histogram. This due to the direct transformation that only considers optimization for human-eye contrast sensitivity. This indicates that better visibility for the human eye does not guarantee better performance in ship detection algorithms. Hence, we did not adopt such a direct transformation approach in the enhancement method.

We verified that the generated image provides excellent visibility for target recognition. For several areas we used the generated high-precision image for evaluating ship detection results, as shown in Fig. 12. Ship detection results were reproduced with the ship size based on pixels. This was performed by connecting the center of the target pixels using drawing functions in Matlab. These pixels determine the shape of ship similar to that visible in the image as shown in Fig. 12. This comparison enables a more specific evaluation for individual targets. In particular, we marked small-sized ships with circles. Overall, Fig. 12 shows that

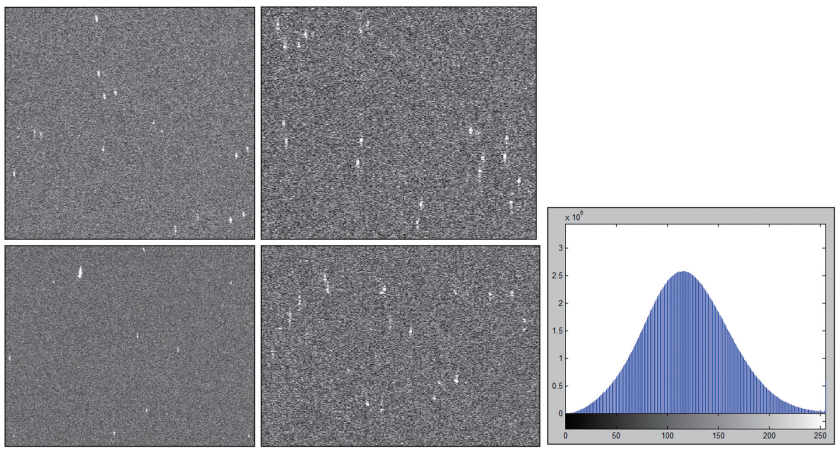

Fig. 11. Sub-images and histogram of a high-precision image obtained by power scaling for the original SAR input data. (Color online only)

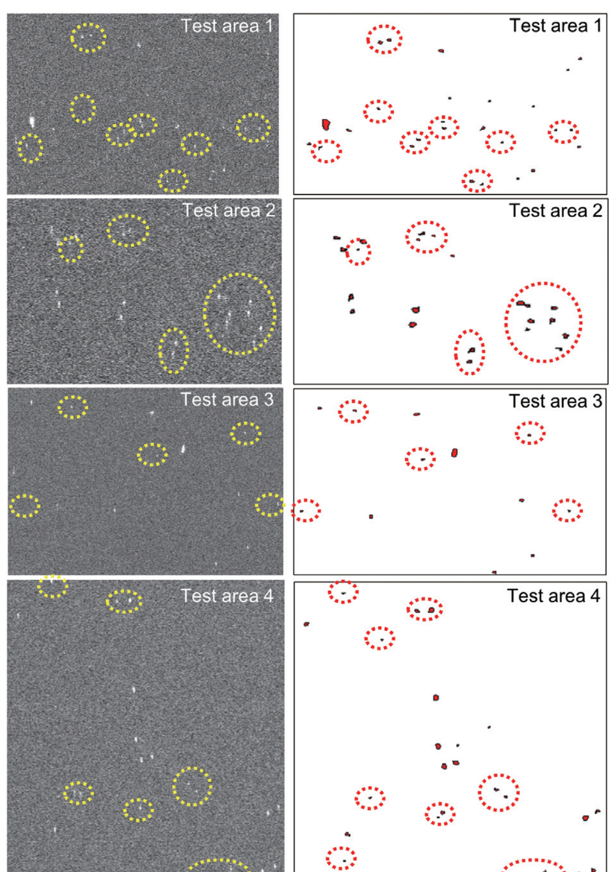

Fig. 12. Visual inspection for ship detection results using the high-precision image. (Color online only)

the targets resulting from our method (right images) were in accordance with those visible in the precision image (left graphic), and obvious commission or omission errors were rarely observed. It could be concluded that our image enhancement method successfully detected ships from the SAR data.

In this section, we describe retrieval of target visibility by generating high-precision images from the SAR input data using direct transformation based on power-law scaling. This direct transformation method is recommended to visually inspect targets. In terms of commercial software or operating systems, such target visibility can serve as useful information for manually extracting ships in case the given algorithm fails to automatically detect the target. It can also be used to evaluate ship detection results, as was done in this work. However, such a direct transformation may incur the loss of important information in double-peak distributions, which may lead to difficulties in detecting targets. Consequently, for the ship detection process, power-law scaling was used to achieve target discrimination from a gray scale image generated using logarithmic and linear transformation. In conclusion, our experiments and results verified the power-law scaling potential for SAR image enhancement, while implicating the importance of accounting for the objective at hand and careful considerations when implementing this approach.

5. CONCLUSION

We proposed an effective automatic image enhancement method for small ship detection and inspection using RADARSAT-2 HV-polarization image data. The SAR input data is transformed into a highly compressed gray scale image with bimodal (double-peaked) distributions for targets and background clutters. Considering such distributions the gray scale image is rescaled based on power-law transformation and then min-max linear stretching, which results in efficient target emphasis and background suppression. The clutter remaining after the contrast adjustment can be removed using a simple median filter. Ship detection can be performed using simple global thresholding because the output image using our enhancement method is close to binary data. In our evaluation of the method, we verified ship detection results with the respective sizes and compared them with ships identified by AIS and with ships visible in a high-precision image generated for target recognition by a human operator.

Previous studies employed complex filters and thresholding algorithms for small ship detection because, in most cases, their primary concerns were to improve the ship detection rate in SAR images. In the present study we devised an enhancement method that does not require such complexity and can be automatically implemented with the intention of developing a near-real-time automatic ship detection and monitoring system. Our method showed outstanding performance for small ship detection using SAR imagery.

We verified that our method: (1) uses highly compressed data for high-speed processing, (2) provides excellent ship visibility, (3) automatically performs SAR image enhancement, (4) does not contain complex filtering or thresholding, and (5) provides a high detection rate for small ships in SAR imagery. Overall, the results in this work support the potential of our approach as an automatic SAR enhancement method for a near-real-time ship detection and inspection system. We demonstrated the potential of power-law scaling for SAR image enhancement. However, it should be noted that this approach was validated with a limited number of datasets and that more quantitative evaluation will be required to thoroughly validate this method. Further method validation will be investigated in future research. We hope that our approach will improve the understanding of automatic image enhancement for ship detection and inspection in SAR data.

Acknowledgements This research was a part of the projects entitled "Development of Ship-handling and Passenger Evacuation Support System", "Construction of Ocean Research Stations and their application Studies, Phase 2", and "Development of Korea Operational Oceanographic System (KOOS), Phase 2" funded by the Ministry of Oceans and Fisheries, Korea, and "Development of fundamental technology for coastal erosion control" of KIOST.

REFERENCES

Chaturvedi, S. K., C. S. Yang, K. Ouchi, and P. Shanmugam, 2012: Ship recognition by integration of SAR and AIS. *J. Navig.*, **65**, 323-337, doi: 10.1017/S0373463311000749. [Link]

Dubey, S., D. Tiwari, O. P. Singh, and K. K. Singh, 2013: Speckle noise removal and enhancement of SAR images. *Int. J. Eng. Adv. Tech.*, **2**, 639-644.

Hong, D. B. and C. S. Yang, 2014: Classification of passing vessels around the Ieodo Ocean Research Station using Automatic Identification System (AIS): November 21-30, 2013. *J. Kor. Soc. Mar. Environ. Energy*, **17**, 297-305, doi: 10.7846/JKOSMEE.2014.17.4.297. [Link]

Huang, S., D. Liu, G. Gao, and X. Guo, 2009: A novel method for speckle noise reduction and ship target detection in SAR images. *Pattern Recogn.*, **42**, 1533-1542, doi: 10.1016/j.patcog.2009.01.013. [Link]

Huang, S. C., F. C. Cheng, and Y. S. Chiu, 2013: Efficient contrast enhancement using adaptive gamma correction with weighting distribution. *IEEE Trans. Image Process.*, **22**, 1032-1041, doi: 10.1109/TIP.2012.2226047. [Link]

Hwang, S. I. and K. Ouchi, 2010: On a novel approach using MLCC and CFAR for the improvement of ship detection by synthetic aperture radar. *IEEE Geosci. Rem. Sens. Lett.*, **7**, 391-395, doi: 10.1109/LGRS.2009.2037341. [Link]

Kim, B. G., D. J. Kim, and D. J. Park, 2001: Novel precision target detection with adaptive thresholding for dynamic image segmentation. *Mach. Vis. Appl.*, **12**, 259-270, doi: 10.1007/s001380050145. [Link]

Margarit, G., J. J. Mallorqui, J. M. Rius, and J. Sanz-Marcos, 2006: On the usage of GRECOSAR, an orbital polarimetric SAR simulator of complex targets, to vessel classification studies. *IEEE Trans. Geosci. Remote Sensing*, **44**, 3517-3526, doi: 10.1109/TGRS.2006.881120. [Link]

Margarit, G., J. J. Mallorquí, J. Fortuny-Guasch, and C. López-Martínez, 2009: Exploitation of ship scattering in polarimetric SAR for an improved classification under high clutter conditions. *IEEE Trans. Geosci. Remote Sensing*, **47**, 1224-1235, doi: 10.1109/TGRS.2008.2008721. [Link]

Ouchi, K., 2013: Recent trend and advance of synthetic aperture radar with selected topics. *Remote Sens.*, **5**, 716-807, doi: 10.3390/rs5020716. [Link]

Ouchi, K., S. Tamaki, H. Yaguchi, and M. Iehara, 2004: Ship detection based on coherence images derived from cross correlation of multilook SAR images. *IEEE Geosci. Rem. Sens. Lett.*, **1**, 184-187, doi: 10.1109/LGRS.2004.827462. [Link]

Wang, C., M. Liao, and X. Li, 2008: Ship detection in SAR image based on the alpha-stable distribution. *Sensors*, **8**, 4948-4960, doi: 10.3390/s8084948. [Link]